

Theoretical Studies of the Ground and Excited States of a Model of the Active Site in Oxidized and Reduced Rubredoxin¹

Raymond A. Bair² and William A. Goddard III*

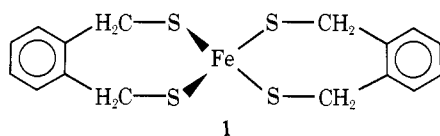
Contribution No. 5743 from the Arthur Amos Noyes Laboratory of Chemical Physics, California Institute of Technology, Pasadena, California 91125. Received February 27, 1978

Abstract: Using the system $\text{Fe}(\text{SH})_4$ to model the active site of rubredoxin, we have carried out ab initio quality Hartree-Fock and extensive configuration interaction studies of the ground and excited states of both the oxidized and reduced systems. We have established that the ground state is high spin in both redox forms and find charge distributions in agreement with Mössbauer studies. Based on calculated excitation energies and intensities, we have assigned all the spectral features below 3 eV including d-d spin-allowed, d-d spin-forbidden, and ligand to metal charge-transfer bands.

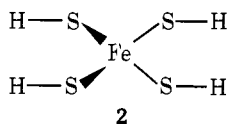
I. Introduction

In recent years nonheme iron-sulfur proteins have been shown to be important in many basic metabolic processes including bacterial nitrogen fixation, mitochondrial electron transport, and photosynthesis.³ Still, the function of many iron-sulfur proteins is unknown. Crystallographic and spectrographic studies of the natural proteins have given hints of the mechanisms involved in several systems; however, it was the development and characterization of accurate model systems that permitted a more detailed understanding of the microscopic processes at the active site of the ferredoxins and rubredoxins.⁴⁻⁶

Perhaps the simplest of the Fe-S proteins is rubredoxin (Rd), which has a single Fe at the active site surrounded tetrahedrally by four cysteine sulfur atoms, with the whole unit at the surface of a small protein⁷ (molecular weight 5000-20 000). Several model systems have been developed by Holm, Ibers, and co-workers⁴ including $[\text{Fe}(\text{S}_2\text{-}o\text{-xyl})_2]$ (where the net charge is -1 for oxidized and -2 for reduced), which we shall hereafter refer to as the Holm-Ibers model. Crystal structures, optical spectra, Mössbauer spectra, and redox potentials were obtained for both the oxidized and reduced forms of the Holm-Ibers model (1).



In order to provide a theoretical foundation for understanding these properties, we have carried out detailed ab initio level theoretical studies of an idealization of 1 where the bond lengths and geometries are based on the Holm-Ibers model. Using 2 we have examined the wave functions and charge



distributions of numerous electronic states of both the oxidized and reduced forms. These calculations include a high level of electron correlation and allow detailed assignments of the electronic spectra, including ligand to metal charge-transfer (LMCT).

II. Calculation Details

A. Geometries. Our model follows the dimensions and angles from the Holm-Ibers model,⁴ which is structurally quite similar to the active site in rubredoxin (Rd).⁷ (The geometric parameters of Rd are known to much less certainty than for

the Holm-Ibers model and are available only for the oxidized form.) Some bond lengths and angles were changed slightly but without significant deviations from the experimental crystal structure. For the oxidized model we also averaged the structures of the two similar anions found in the crystal.

Specifically, the parameters of the *oxidized* model were taken as follows. The Fe-S bond length was set to the average distance of 2.267 Å. The average Fe-S bond length from early x-ray crystallographic studies of oxidized Rd is 2.24 Å,⁷ whereas more recent x-ray studies indicate an average bond length of 2.28 Å. From studies of extended x-ray absorption fine structure (EXAFS),^{7c,d} Bunker and Stern have concluded that the average FeS bond length of oxidized Rd and oxidized Holm-Ibers model are both 2.267 ± 0.003 Å. The S1-Fe-S2 and S3-Fe-S4 angles were chosen as 110° , again, the average of these angles in the model compound. (In the model compound, S1 and S2 are part of a bidentate ligand, as are S3 and S4.) The dihedral angle of the S1-Fe-S2 and S3-Fe-S4 planes was taken as 90° since the observed angles of 92.3° and 92.7° were so close to ideal. The Fe-S-H bond angle of 101.5° is the average of the observed Fe-S-C angles. The four H atoms were each moved 48.4° out of the S1-Fe-S2 and S3-Fe-S4 planes. The corresponding angle in the experimental crystal structure varied from 39.8° to 54.7° . The S-H bond length was chosen as in H_2S , 1.33 Å.

The same procedure was used to obtain the angles and distances for the *reduced* model. The Fe-S distance was increased to 2.356 Å; the S-H distance was retained as 1.33 Å. The S1-Fe-S2 and S3-Fe-S4 angles were 111.4° , the Fe-S-H angles were 108.2° , the S1-Fe-S2 and S3-Fe-S4 dihedral angle remained 90° , and the H atoms were placed 20.7° out of the corresponding S-Fe-S plane.

Our models are drawn in Figure 1. As discussed later, the most strongly bound d orbital for both oxidized and reduced models is of d_{z^2} character (cigar-like); however, the axis of this orbital is different in the two states. For simplicity in discussion we have chosen the z axis (see Figure 1) of each form to be the axis of this d_{z^2} -like orbital. Neither of the $\text{Fe}(\text{SH})_4$ models has any symmetry elements. In the oxidized form, the d_{z^2} orbital of the SCF sextet ground state is along the bisector of the S1-Fe-S3 and S2-Fe-S4 planes. This is probably due to the large angle of 48.4° between the H1-S1-S2-H2 and S1-Fe-S2 planes (an angle of 0° would give the molecule D_{2d} symmetry). The strong interaction of S lone pairs with the Fe d orbitals determines the orientation of the d orbitals. However, in the reduced model this same dihedral angle is only 20.7° (much closer to the D_{2d} limit) and consequently the d_{z^2} orbital shifts to the axis formed by the bisector of the S1-Fe-S2 and S3-Fe-S4 planes. Therefore, although all the bonds in both

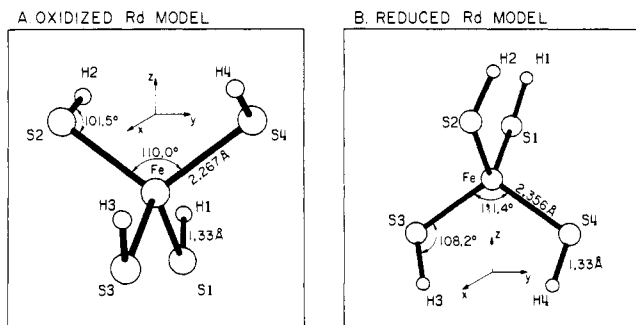


Figure 1. Geometries of the oxidized and reduced model complex.

the oxidized and reduced models have the same relative orientation, the drawings in Figure 1 have been made so that the Fe *d* orbitals (of the SCF Hamiltonians) are congruent.

B. Wave Functions. We carried out Hartree-Fock (HF)⁸ and configuration interaction (CI) calculations on each geometry. On Fe we used a valence double- ζ contraction of the Wachters (14s, 8p, 5d) primitive Gaussian basis⁹ with the Ar core electrons replaced by an ab initio quality effective potential.¹⁰ A set of diffuse p functions ($\alpha = 0.09$) was also included on the Fe center. Thus the Fe basis consisted of 18 contracted basis functions (3s, 1p 2d). For the S we used a valence double ζ contraction of the Huzinaga (11s, 7p) primitive Gaussian basis and included an ab initio effective potential to replace the Ne core electrons,¹¹ leading to a total of nine contracted functions (3s, 2p) on each S center. The H atom basis was a double- ζ contraction of the Huzinaga¹² (4s) Gaussian basis ($\zeta = 1.2$), bringing the total Fe(SH)₄ basis set to 62 contracted functions. The integrals were evaluated using the POLYATOM¹³ program, and the HF calculations were carried out with the GVB TWO¹⁴ program.

The open-shell SCF wave functions calculated for our models may be considered as the antisymmetrized product of two parts, the doubly occupied valence orbitals (Φ_{CS}) and the singly occupied valence orbitals (Φ_{OS}):

$$\psi = \mathcal{A}[\Phi_{CS}\Phi_{OS}] \quad (1)$$

For example, in the sextet state, the closed-shell part may be expanded as the product of 16 doubly occupied orbitals

$$\Phi_{CS} = \phi_1(1)\phi_1(2)\phi_2(3)\phi_2(4) \dots \phi_{16}(31)\phi_{16}(32)\alpha\beta\alpha\beta\alpha\beta \dots \quad (2)$$

mainly localized on the ligands, and the open-shell part as the product of five singly occupied orbitals, mainly of *d* character on the Fe and with parallel spin:

$$\Phi_{OS}^{\text{sextet}} = \phi_{17}(33)\phi_{18}(34)\phi_{19}(35) \times \phi_{20}(36)\phi_{21}(37)\alpha\alpha\alpha\alpha\alpha \quad (3)$$

In these calculations, no restriction has been placed on the shape or localization of any of these 21 orbitals, and no symmetry was used.

For the reduced quintet SCF, we solved first for an averaged *d*⁶ state, where the variational Hamiltonian (Fock operator) was derived from the average energy of the five possible quintet configurations

$$\Phi_{OS}^{\text{quintet}} = \phi_{17}(33)\phi_{18}(34)\phi_{19}(35)\phi_{20}(36) \times \phi_{21}(37)\phi_n(38)\alpha\alpha\alpha\alpha\alpha\beta \quad (4)$$

(where $n = 17, 18, 19, 20$, or 21). Starting with any particular configuration [say, $n = 17$ in eq 4] constructed with this set of optimum orbitals from the average wave functions and including all single excitations (using an appropriate set of virtual orbitals) leads to an energy within 0.01 eV of the energy obtained by solving self-consistently for the orbitals of the same

configuration. The reason for using this procedure is to have a set of orbitals for the CI calculations not biased toward any particular *d*⁶ configuration.

In these CI calculations the various configurations were constructed from 26 orthogonal functions consisting of the 21 occupied orbitals from the SCF calculations, plus a set of five diffuse *d* virtual orbitals localized on Fe (26 functions in all). The configuration list contained all singles and selected double excitations from the dominant configurations of the state being calculated. More detail on the method used to generate the configuration list is in the Appendix. No symmetry was used in the CI calculations.

III. Results of Reduced States

Our calculations indicate that the ground state of reduced Rd can be accurately described as ferrous *d*⁶ Fe. Ferrous Fe can have three possible spins, high spin ($S = 2$ or quintet), intermediate spin ($S = 1$ or triplet), or low spin ($S = 0$ or singlet). Our calculations lead to a high spin or quintet ground state. This is in agreement with experimental observations^{15,16} and our previous calculations¹⁷ on three other geometries. The lowest triplet and singlet states are found at 2.79 and 4.03 eV, respectively, above the quintet ground state. The results for the CI calculations are given in Table I.

A. Quintet *d*⁶ States. 1. Energy Levels. There are five possible quintet reduced states, depending upon which of the five *d* orbitals is doubly occupied. In T_d symmetry these states would be split into ⁵E and ⁵T₂ states with ⁵E lower and a separation of 0.43 eV. In the lower symmetry of our complex, the ⁵E state is split into two states (denoted as *d*_z and *d*_{x²-y²}) separated by 0.17 eV and the ⁵T₂ state is split into three levels separated by a total of 0.30 eV, as indicated in Figure 2. We find that the ground state has the *d*_z orbital doubly occupied where this orbital is oriented as in Figure 1. As will be discussed in section V, the quadrupole splitting from Mössbauer studies is in excellent agreement with these results. Some of the orbitals for the ground state are plotted in Figures 3 and 4.

Since the transitions to the *d*_{xz} and *d*_{yz} orbitals are split by only 0.01 eV in our calculation, spin-orbit coupling is expected to be an important factor, increasing this separation. For our estimation of the spin-orbit contribution to the splitting of the 0.61- and 0.62-eV states, we considered the application of the atomic spin-orbit coupling constant $\lambda = 400 \text{ cm}^{-1}$ to an atomic wave function having *d*-*d* states at the same relative energies. The spin-orbit matrix element

$$\lambda \langle \psi_{yz} | \mathbf{L} \cdot \mathbf{S} | \psi_{xz} \rangle \quad (5)$$

between these two states is estimated to be 0.025 eV (200 cm^{-1}), which moves the 0.61- and 0.62-eV transitions to 0.585 and 0.645 eV, respectively (4720 and 5200 cm^{-1}). A complete treatment of the spin-orbit coupling for the Fe(SH)₄²⁻ molecular wave functions should give a smaller matrix element (one source of the decrease is the reduction of the effective λ in the molecular case). Thus, we expect that spin-orbit effects would account for at most a total splitting of 0.06 eV in the two highest ⁵T₂ components (*d*_{yz} and *d*_{xz} doubly occupied) and would not shift the lower ⁵T₂ component (*d*_{xy} doubly occupied, 0.32 eV).

The first excited quintet state has the *d*_{x²-y²} orbital doubly occupied and corresponds to the second component of the ⁵E state. The excitation energy is 0.17 eV (1370 cm^{-1}); however, this transition is dipole forbidden (calculated oscillator strength $f = 2.5 \times 10^{-8}$). The temperature dependence of the Mössbauer quadrupole splitting leads to an estimate of 0.11 eV (900 cm^{-1})⁴ for this *d*_z-*d*_{x²-y²} separation in the Holm-Ibers model, in reasonable agreement with our calculations. (Eaton and Lovenberg¹⁸ estimate $\sim 850 \text{ cm}^{-1}$ from the Mössbauer studies on Rd by Phillips et al.¹⁵).

The next three excited states correspond to components of

Table I. Excited States of the Reduced Model, $\text{Fe}(\text{SH})_4^{2-}$ (Energies in eV)

| state | d configuration | | | | | $\text{Fe}(\text{SH})_4^{2-}$ calculated | | | $(\text{Et}_4\text{N})_2[\text{Fe}(\text{S}_2\text{-o-xy})_2]^a$ | | rubredoxin ^b | | |
|-------|-----------------|-------------|------|------|------|--|-----------------|------------------------|--|-------------------|---|------------------------------|---|
| | z^2 | $x^2 - y^2$ | xy | yz | xz | spin | transition type | excitation energy (CI) | oscillator strength (f) | excitation energy | ϵ , $\text{M}^{-1} \text{cm}^{-1}$ | excitation energy | ϵ , $\text{M}^{-1} \text{cm}^{-1}$ |
| I | 2 | 1 | 1 | 1 | 1 | 2 | g.s | 0 ^c | | | | | |
| II | 1 | 2 | 1 | 1 | 1 | 2 | d-d | 0.17 | 2.5×10^{-8} | $\sim 0.11^d$ | | $\sim 0.11^d$ | |
| III | 1 | 1 | 2 | 1 | 1 | 2 | d-d | 0.32 | 1.1×10^{-4} | | | ≤ 0.50 | |
| IV | 1 | 1 | 1 | 2 | 1 | 2 | d-d | 0.61 | 1.6×10^{-4} | ≤ 0.62 | 109,sh | 0.68-0.87 | 130 |
| V | 1 | 1 | 1 | 1 | 2 | 2 | d-d | 0.62 | 1.6×10^{-4} | 0.69 | 123 | $(f = 9.6 \times 10^{-4})^b$ | |
| VI | 2 | 2 | 1 | 1 | 0 | 1 | d-d | 2.79 | } | 2.6-3.0 | 390 | | |
| VII | 2 | 2 | 1 | 0 | 1 | 1 | d-d | 2.80 | | | | | |
| VIII | 2 | 1 | 2 | 0 | 1 | 1 | d-d | 2.97 | | | | | |
| IX | 2 | 1 | 2 | 1 | 0 | 1 | d-d | 2.99 | | | | | |
| X | 2 | 2 | 0 | 1 | 1 | 1 | d-d | 3.03 | | | | | |
| XI | 2 | 2 | 2 | 0 | 0 | 0 | d-d | 4.03 | | | | | |

^a 0.62 and 0.69 bands in MeCN, 2.6-3.0 band in DMF; ref 4. ^b *C. pasteurianum*. D_2O ; ref 19. ^c Total energy -65.2748 hartrees (CI). Energy of SCF calculation -65.2441 hartrees (averaged over the five quintet states; see text). ^d Estimated from the temperature dependence of the quadrupole splitting $\Delta E_Q(T) = \Delta E_Q(0) \tanh(\Delta 2kT)$, ref 4 and 18.

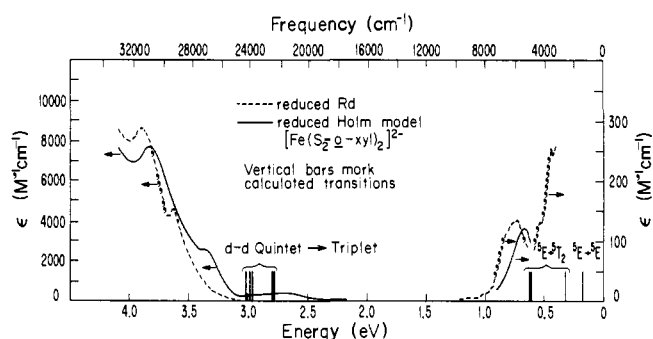


Figure 2. Comparison of calculated transitions with experimental spectra for the reduced model, $\text{Fe}(\text{SH})_4^{2-}$. The calculated, spin-allowed d-d transitions fall between 0.34 and 0.67 eV, while the spin-forbidden d-d transitions are calculated to be between 2.79 and 3.03 eV (vertical bars). The Rd spectrum is from ref 19 (0-1.6 eV) and ref 4 (1.6-4 eV). The Holm-Ibers model spectrum is from ref 4.

the $^5\text{T}_2$ state (either d_{xy} , d_{yz} , or d_{xz} doubly occupied), all of which are dipole allowed from the ground state. Of these, d_{xy} is the lowest with an excitation energy of 0.32 eV (2580 cm^{-1}), while d_{yz} and d_{xz} are at 0.61 (4920 cm^{-1}) and 0.62 eV (5000 cm^{-1}), respectively.

The calculated oscillator strengths for these three states are 0.000 11, 0.000 16, and 0.000 16, respectively. The measured value is 0.000 96 for the 0.69-eV transition in Rd.¹⁹ Later we will quote estimations of f values from experimental spectra where we use the peak absorbance and half-width from the spectra and calculate the area of the corresponding Gaussian line shape. Using this procedure for the 0.69-eV peak of the Rd spectra leads to $f = 0.0011$, in good agreement with the value (0.000 96) quoted by the experimentalists; this supports the simple method of estimation. Considering this observed transition to be the composite of our two calculated transitions at 0.61 and 0.62 eV, the sum of the two oscillator strengths is 0.000 32, which is a factor of 3 smaller than the observed value. This is an acceptable level of agreement considering that we have calculated only the electric dipole contribution to the intensity. This weak transition may gain intensity from mechanisms we have not explicitly included in our calculation, such as magnetic dipole or electric quadrupole terms. These possibilities are being investigated.

2. The Splittings of the Tetrahedral Levels. The S atoms of our complex are almost tetrahedral, and the splittings of the ^5E and $^5\text{T}_2$ states found above are nearly entirely due to the orientation of the S-H bonds (cysteine S-C_β bonds in the protein). The reason why the second nearest neighbors have

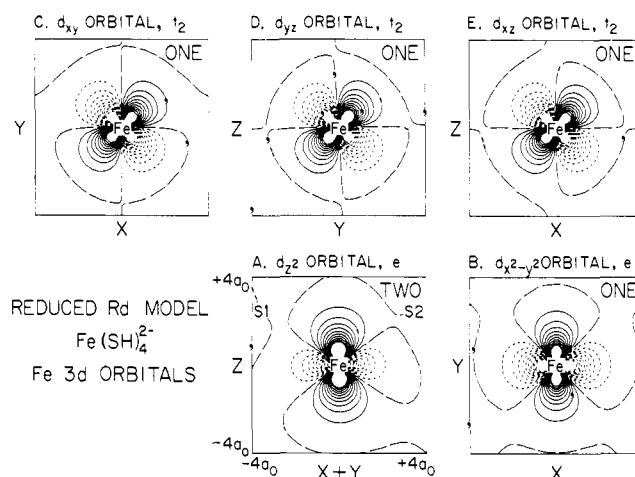


Figure 3. Amplitudes of the d orbitals for the quintet ground state of the reduced model, $\text{Fe}(\text{SH})_4^{2-}$. Long dashes indicate zero amplitude; solid and dotted lines indicate positive and negative amplitude (separation of adjacent contours is 0.05 au). In this state, four d orbitals are singly occupied, while the d_{z^2} orbital is doubly occupied.

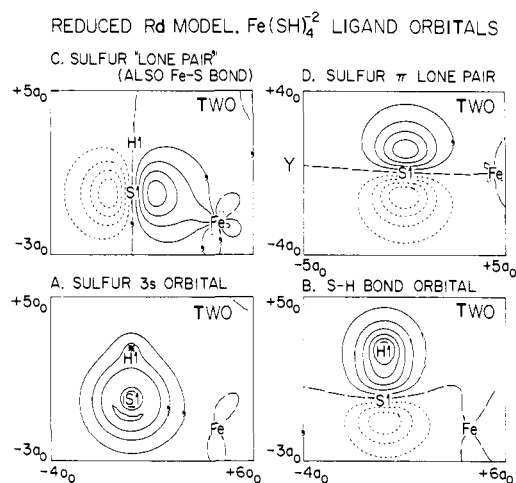


Figure 4. Amplitudes of the localized ligand orbitals of the quintet ground state of the reduced model, $\text{Fe}(\text{SH})_4^{2-}$. Contours are plotted in the same manner as in Figure 3. All four ligand orbitals are doubly occupied.

such an effect on the Fe orbitals is that the orientation of the S-H bond restricts the orientation of the two lone pairs on each S which in turn interact strongly with the Fe. Thus orientation of these Fe-S- C_β angles may play an important part in de-

termining the redox properties of the Fe site in rubredoxin and in the model system.

3. Experimental Energy Levels. Averaging the two 5E components and the three 5T_2 components leads to a $10Dq$ of 0.43 eV (3500 cm^{-1}). In comparing this value with experiment, we encounter the difficulty that for both Rd and most model systems spectra are not available in the region of 0.2–0.6 eV so that some of the d–d transitions are not observed. One exception is the compound $\{[(\text{CH}_3)_2\text{PS}]_2\text{N}\}\text{Fe}^{\text{II}}$ synthesized by Davison and Switkes,²⁰ which shows three d–d absorption bands at 0.38 (3100 cm^{-1}), 0.51 (4098 cm^{-1}), and 0.62 eV (5000 cm^{-1} , sh), with extinction coefficients of 101, 108, and 70 $\text{M}^{-1} \text{cm}^{-1}$, respectively. Our calculations indicate that the transitions from d_{z^2} to the three t_2 levels should have almost equal intensities and hence we assign these three peaks as the three $d_{z^2} \rightarrow t_2$ transitions, leading to an experimental position for the average 5T_2 state of 0.50 eV (above d_{z^2}). Assuming the theoretical value of 0.17 eV for the separation between the 5E components leads thus to a value of 0.42 eV (3400 cm^{-1}) for the ligand field splitting in the Davison and Switkes compound. This is in excellent agreement with our theoretical calculations (0.43 eV) and is also consistent with their Co^{II} derivative which has $10Dq = 0.47$ eV (3831 cm^{-1}). (In general Co^{II} should show a slightly larger $10Dq$ than Fe^{II} .)

Comparison of our results with the experimental spectra of Rd and the model compounds is difficult because the dipole-allowed d–d transitions are in a range (0.3–0.7 eV) that is difficult to examine experimentally. The difficulties are twofold: (1) detectors are inadequate and may cover only a part of the range and (2) the infrared transitions of many common solvents fall in this region. Consequently spectra are not available below 0.5 eV for Rd or below 0.68 eV for the Holm–Ibers model. We expect a dipole-allowed transition in this region for Rd and for the Holm–Ibers model. A strong indication that the reported spectra do miss some transitions is the very large values of $10Dq$ (5000–6250 cm^{-1}) obtained from analysis of these spectra^{4,19} when it is assumed that all allowed transitions are observed. Such values are inconsistent with the results of Davison and Switkes, the theoretical results, and the results on the Co^{II} derivative of the Holm–Ibers model which has a $10Dq$ of about 4200 cm^{-1} (0.52 eV) (the value for Co^{II} should be slightly larger than the Fe^{II} model). The presence of an undetected band at 0.3–0.4 eV (corresponding to our calculated transition at 0.32 eV) would move the experimental $10Dq$ back to a reasonable value.

The theoretical results indicate that excitations to all three t_2 orbitals should be comparable in strength and this was found experimentally for the Davison and Switkes model.²⁰ Since the intensity (ϵ 130) of the highest band in Rd¹⁹ (0.68–0.86 eV) and the intensity (ϵ 123) of the highest band in the Holm–Ibers model⁴ (0.69 eV) are comparable, we suggest that there are one or two additional lower energy bands for both systems (depending upon a possible degeneracy), one of which is partially observed at 0.5 eV in Rd.

In summary, our calculated transitions and intensities are in excellent agreement with current experimental results (Table I). The crucial test of our assignments would be to detect the low-energy ~ 0.32 -eV transition. Perhaps absorption experiments on single crystals with polarized light (or MCD) would allow the transition to be detected.

B. Higher States. The next group of states was found at 2.79–3.02 eV (22 500–24 400 cm^{-1}). These states are triplet with d^6 character and are spin forbidden from the ground quintet states. Experimentally, Holm and co-workers⁴ find a weak band (ϵ 390) at 2.6–3.0 eV in their model compound. This is approximately the same intensity as found for spin-forbidden d–d transitions in their oxidized model. (We have not calculated oscillator strengths for these transitions since they require inclusion of spin–orbit coupling.) Owing to this agreement of

excitation energy and intensity, we assign the 2.6–3.0-eV band as quintet \rightarrow triplet d–d transitions.

The first singlet d^6 state was found at 4.03 eV (32 500 cm^{-1}) above the quintet ground state. The transitions to these states from the ground state should be very weak and are probably not detected.

We carried out calculations sufficient to describe ligand to metal charge transfer (LMCT) but found none lower than 5 eV (for the oxidized model such transitions are at 2 and 2.5 eV). To describe metal to ligand charge transfer (MLCT) requires a good treatment of excited ligand orbitals and we have not carried out such calculations. Experimentally, transitions that could possibly be MLCT are observed at 3.0–3.8 eV in both oxidized and reduced systems.¹⁹

In summary, for the reduced model we have accounted for the observed spectral features at 0.3–0.8 (d–d dipole allowed) and 2.6–3.0 eV (d–d spin forbidden). There are also features at 3.4–3.8 eV which could be MLCT.

IV. Results on Oxidized States

The usual description of the oxidized ferric Fe is in terms of d^5 configurations leading to high spin ($S = 5/2$ or sextet), intermediate spin ($S = 3/2$ or quartet), or low spin ($S = 1/2$ or doublet). As for the reduced case, we find a high-spin ground state in agreement with numerous experimental results (e.g., magnetic susceptibility,¹⁵ ESR,²¹ Mössbauer¹⁶). The calculated energies for various states are included in Table II. The lowest quartet state is 0.98 eV (7900 cm^{-1}) above the sextet while the lowest doublet state is 2.76 eV (22 300 cm^{-1}) above the ground state.

A. The Sextet Ground State. In the reduced ground state, the wave function was qualitatively the same as the usual picture of a d^6 ferrous Fe. To be sure there is some delocalization of Fe d orbitals onto the ligands, but nothing of qualitative significance. However, the oxidized sextet ground state differs considerably from the simple picture of a d^5 Fe. We find that the final CI wave function can be described as about 20% $\text{Fe}^{3+}\text{L}_4^{4-}$ and about 80% $\text{Fe}^{2+}\text{L}_4^{3-}$ where $\text{L}_4^{4-} \equiv (\text{HS})_4$. The $\text{Fe}^{3+}\text{L}_4^{4-}$ term represents the usual ferric d^5 Fe, corresponding to oxidizing an electron from the doubly occupied d_{z^2} orbital of the reduced ground state. Here the $\text{Fe}^{2+}\text{L}_4^{3-}$ term is in fact a superposition of three important terms which can be written as

$$\begin{aligned} & [(d_{z^2})^1(d_{x^2-y^2})^1(d_{xy})^1(d_{xz})^1(d_{yz})^2](l_{xy})^2(l_{xz})^2(l_{yz})^1 \\ & + [(d_{z^2})^1(d_{x^2-y^2})^1(d_{xy})^1(d_{xz})^2(d_{yz})^1](l_{xy})^2(l_{xz})^1(l_{yz})^2 \\ & + [(d_{z^2})^1(d_{x^2-y^2})^1(d_{xy})^2(d_{xz})^1(d_{yz})^1](l_{xy})^1(l_{xz})^2(l_{yz})^2 \end{aligned} \quad (6)$$

The first term corresponds qualitatively to exciting an electron from a ligand orbital of yz symmetry into the ferric d_{yz} orbital. The second and third terms represent similar excitations into the d_{xz} and d_{xy} orbitals, respectively. In addition, there are smaller terms which correspond to excitations into the d_{z^2} and $d_{x^2-y^2}$ orbitals. Thus, comparing with the reduced system, the extra hole resulting from oxidation is delocalized over the Fe and ligands so that only about 20% is on the Fe while about 80% is spread equally over the four ligands.

A salient diagnostic feature of high-spin d^5 Fe is a spherically symmetric charge distribution. As discussed in more detail in section V, the observed electric field gradient (from Mössbauer studies) of oxidized iron is much smaller than that of reduced iron with the ratio being

$$q_{\text{ox}}/q_{\text{red}} = -0.17 \quad (7)$$

for the Holm–Ibers model.⁴ Our calculated ratio is -0.24 , in reasonable agreement with the experimental results.

B. Quartet Excited States. In the oxidized system the first four excited states are quartets. They correspond to exciting

Table II. Excited States of the Oxidized Model, Fe(SH)₄⁻ (Energies in eV)

| state | d configuration | | | | | Fe(SH) ₄ ⁻ calculated | | | | (Et ₄ N)[Fe(S ₂ -o-xyI) ₂] ^a | | rubredoxin ^b | |
|-----------------|-----------------|---------------------------------|----|---------|----------------------|---|-----------------|------------------------|-------------------------|---|-------------------------------------|-------------------------|-------------------------------------|
| | z ² | x ² - y ² | xy | xz + yz | xz - yz ^c | spin | transition type | excitation energy (CI) | oscillator strength (f) | excitation energy | ε, M ⁻¹ cm ⁻¹ | excitation energy | ε, M ⁻¹ cm ⁻¹ |
| I | 1 | 1 | 1 | 1 | 1 | 5/2 | g.s. | 0 ^d | | | | | |
| II | 2 | 1 | 1 | 1 | 0 | 3/2 | d-d | 0.98 | | | | | |
| III | 1 | 2 | 1 | 1 | 0 | 3/2 | d-d | 1.08 | | | | | |
| IV | 1 | 1 | 2 | 1 | 0 | 3/2 | d-d | 1.44 | | | | | |
| V | 1 | 1 | 1 | 2 | 0 | 3/2 | d-d | 1.58 | | | | 1.66 | 360 |
| VI | 1 | 1 | 1 | 1 | 1 | 3/2 | spin flip | 1.90 | | | | | (f = 0.0025) ^b |
| VII | 2 | 1 | 1 | 1 | 1 | 5/2 | LMCT | 2.06 | 0.024 | 1.8-2.0 | 1500 | 2.2 | ~4000 |
| VIII | 1 | 2 | 1 | 1 | 1 | 5/2 | LMCT | 2.12 | 0.009 | | | | |
| IX ^e | 1 | 1 | 2 | 1 | 1 | 5/2 | LMCT | 2.32 | 0.007 | | | | |
| X | 1 | 1 | 1 | 0 | 2 | 3/2 | d-d | 2.46 | | | | | |
| XI ^e | 1 | 1 | 2 | 1 | 1 | 5/2 | LMCT | 2.46 | 0.024 | 2.55 | 5400 | 2.53 | 8850 |
| XII | 1 | 1 | 1 | 2 | 1 | 5/2 | LMCT | 2.55 | 0.024 | | | | |
| XIII | 2 | 2 | 1 | 0 | 0 | 1/2 | d-d | 2.76 | | | | | (f = 0.13 ± 0.06) ^f |

^a 4:1 Me₂SO/H₂O v/v, aqueous portion 50 mM TrisCl, pH 8.5; ref 4. ^b *C. pasteurianum*. H₂O; ref 4. ^c Considerable ligand character is also present; see text. ^d Total energy -65.3363 hartrees (CI). SCF energy -65.2729 hartrees. ^e These two states have similar Fe character but differing ligand character. ^f Oscillator strength (*f*, unitless) may be related to absorbance (ε, M⁻¹ cm⁻¹) by $f = 4.315 \times 10^{-9} \int \epsilon(\bar{\nu}) d\bar{\nu}$.

the highest energy unpaired electron of the ground state into each of the four other orbitals containing an unpaired electron. These four states are calculated at 0.98, 1.08, 1.44, and 1.58 eV (7900, 8700, 11 600, and 12 700 cm⁻¹). Rubredoxin exhibits a band in this range (1.5-1.8 eV) with a molar extinction coefficient ε 360 M⁻¹ cm⁻¹.¹⁹ There is no observed absorption in this region in the Holm-Ibers model. The extinction coefficient is comparable in intensity to the transitions we have assigned as d-d spin forbidden in the reduced model, and we assign the band at 1.66 eV in oxidized Rd as d-d spin forbidden (sextet → quartet). This band has been previously assigned as a ⁴T₁ ← ⁶A₁ d-d transition by Rawlings et al.²²

C. Charge Transfer States. In order to examine the possibility of ligand to metal charge transfer (LMCT) we carried out appropriate CI calculations, described in detail in the Appendix. The result was LMCT transitions at 2.06 (16 600 cm⁻¹, *f* = 0.024) and 2.12 eV (17 100 cm⁻¹, *f* = 0.009), each of which involve excitations from the highest occupied ligand π orbital to a singly occupied Fe e-like orbital. (By a ligand π orbital, we mean an orbital delocalized over the various ligands but π-like with respect to each local Fe-S-H plane.) The next higher LMCT transitions were found at 2.32 (18 700 cm⁻¹, *f* = 0.007), 2.46 (19 800 cm⁻¹, *f* = 0.024), and 2.55 eV (20 600 cm⁻¹, *f* = 0.024), each of which are LMCT from occupied ligand π orbitals to Fe t₂-like orbitals.

Experimentally the first transitions strong enough to be charge transfer are observed at 2.2 eV (ε ~4000) in oxidized Rd¹⁹ and at 1.8-2.0 eV (ε 1500) in the Holm-Ibers model.⁴ From the spectra of the Holm-Ibers model we estimate an oscillator strength of *f* = 0.05 ± 0.03. Thus the position and intensity²³ are in good agreement with the theoretical results (Figure 5) and we assign the 1.8-2.0-eV band as LMCT (with the transfer into e-like metal orbitals).

The next higher absorption bands are observed at 2.53 eV in Rd and 2.55 eV in the Holm-Ibers model (with ε 8850 and 5400, respectively). From these spectra we estimate *f* = 0.13 ± 0.06. Thus the calculated position (2.46 and 2.55 eV) and intensity (*f* = 0.049) of these LMCT transitions allow us to assign the peak at 2.5 eV as LMCT where the transition is into the t₂-like metal orbitals.

The above assignments account for all observed spectra below 3 eV. We have not studied the higher states.

V. Detailed Discussions

A. Mössbauer Results. From Mössbauer studies of reduced

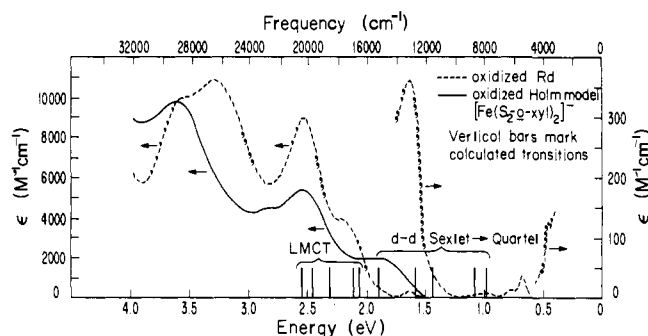


Figure 5. Comparison of calculated transitions with experimental spectra for the oxidized model, Fe(SH)₄⁻. The calculated, spin-forbidden d-d transitions are between 0.98 and 1.90 eV, while the LMCT transitions are calculated to fall between 2.06 and 2.55 eV (vertical bars). The Rd spectrum is from ref 19 (0-1.6 eV) and ref 4 (1.6-4 eV). The Holm-Ibers model spectrum is from ref 4.

Rd¹⁶ and the reduced Holm-Ibers model,⁴ the *V*_{zz} component of the electric field gradient is negative. This is consistent with our calculations which lead to a high-spin d⁶ ground-state configuration with the Fe d_{z²} orbital doubly occupied.

The experiments show a single quadrupole doublet with a splitting energy

$$\Delta E_q = aQ \left(1 + \frac{\eta^2}{3}\right)^{1/2} V_{zz} \quad (8)$$

composed of the constant *a*, the nuclear quadrupole moment, *Q*, of the Mössbauer excited state (*I* = 3/2) of ⁵⁷Fe, the asymmetry parameter $\eta = (V_{xx} - V_{yy})/V_{zz}$, and the electric field gradient *V*_{zz}. Experimentally *Q* is not well known (values range from 0.16 to 0.34 with 0.20 ± 0.03 being perhaps the most reasonable estimate).²⁴ For calculations such as ours in which the core electrons of the Fe are treated as closed shell (or replaced by effective potentials), a correction (called the Sternheimer correction, *R*) is usually applied to the calculated components of the electric field gradient. This accounts for the polarization of the core electrons due to the asymmetric field of the valence electrons and the resulting effect of this polarization upon *V*_{zz}. A common value for this correction reduces *V*_{zz} by 32%; however, there seems to exist little justification for this value. In order to obtain the data required for estimating the Sternheimer correction *R*, we carried out calcu-

Table III. Electric Field Gradients of the Rd Model

| | field gradient, ^a au | | | | au $V_{zz} \times$ $(1 +$ $(\eta^2/3))^{1/2}$ |
|--|---------------------------------|----------|----------|----------|--|
| | V_{xx} | V_{yy} | V_{zz} | η^b | |
| reduced model quintet ground state | 1.35 | 1.00 | -2.35 | 0.15 | -2.36 |
| oxidized model sextet ground state | -0.48 | -0.02 | 0.50 | 0.92 | 0.56 |

^aThe field gradient $V_{\alpha\beta}$ (where $\alpha, \beta = x, y, \text{ or } z$) = $-e\langle\psi|(3r_\alpha r_\beta - \delta_{\alpha\beta}r^2)/r^5|\psi\rangle$. ^bAsymmetry parameter, $\eta = (V_{xx} - V_{yy})/V_{zz}$.

lations of V_{zz} for the ground state (⁵D) of Fe atom. The result was

$$V_{zz} = 2.49 \quad (9)$$

(with no contribution from the core electrons). If there were an experimental value of the quadrupole splitting of atomic Fe for some isotope with $I \geq 1$, the use of eq 8 would lead to an experimental V_{zz} and comparison with eq 9 would lead to a Sternheimer correction

$$V_{zz}^{\text{exptl}} = (1 - R)V_{zz}^{\text{calcd}} \quad (10)$$

(there would be, of course, an uncertainty in R of the same magnitude as the experimental uncertainty in Q). Alternatively, we could calculate the Sternheimer correction by explicitly allowing the core electrons to polarize. This calculation is underway but not complete. Since R is expected to be independent of the state of the valence electrons, we can use the same value for various oxidized and reduced states. In the absence of a reliable value for R , we will compare our calculations with experimental results by taking ratios,

$$\frac{\Delta E_Q^{\text{ox}}}{\Delta E_Q^{\text{red}}} = \frac{\left(1 + \frac{\eta_{\text{ox}}^2}{3}\right)^{1/2} V_{zz}^{\text{ox}}}{\left(1 + \frac{\eta_{\text{red}}^2}{3}\right)^{1/2} V_{zz}^{\text{red}}} \quad (11)$$

where the calculated V_{zz} does not include the effects of core polarization (a , R , and Q cancel out).

For the reduced ground state of our model complex we obtain

$$\left(1 + \frac{\eta_{\text{red}}^2}{3}\right)^{1/2} V_{zz}^{\text{red}} = -2.36 \quad (12)$$

Thus, putting the four SH ligands around the Fe decreases the electric field gradient by only 5% from the value for the atomic ground state, confirming the validity of the d^6 description of the reduced model. For the oxidized state we find

$$\left(1 + \frac{\eta_{\text{ox}}^2}{3}\right)^{1/2} V_{zz}^{\text{ox}} = 0.56 \quad (13)$$

and therefore

$$\Delta E_Q^{\text{ox}}/\Delta E_Q^{\text{red}} = -0.235$$

This compares favorably with the ratio from the Holm model⁴ of -0.17 . Unfortunately, there is some uncertainty in the experimental quadrupole splitting of oxidized Rd;¹⁵ the available data produce a ratio of -0.23 . The large hyperfine splitting usually observed in oxidized Rd Mössbauer spectra¹⁶ makes determination of the quadrupole splitting difficult.

In summary, our calculations provide a theoretical description of the electronic structure consistent with the observed Mössbauer data. The calculated components of these electric field gradients are listed in Table III.

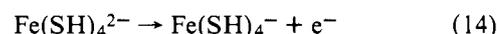
B. Other Calculations. 1.X α . Recently, Norman and Jackels²⁵ employed the SCF-X α scattered wave method in studies of FeS_4^{5-} , $\text{Fe}(\text{SH})_4^-$, and $\text{Fe}(\text{SCH}_3)_4^-$ as models of oxidized Rd. They reported results only for the sextet ground state. Their calculations on $\text{Fe}(\text{SH})_4^-$ were carried out using both spin-restricted and spin-polarized X α wave functions. The ordering of the d orbitals in the spin-polarized calculation is the same as found in this work: $z^2 < x^2 - y^2 < xy < xz, yz$. They find that the highest energy occupied orbital has about 80% ligand character. This is analogous to our observation that the CI wave function for the oxidized ground state is a superposition of three important terms which produce a wave function with 80% $\text{Fe}^{2+}\text{L}_4^{3-}$ character.

2. Extended Hückel Theory. A more extensive study of the properties of the active site of Rd was made by Loew and co-workers.^{26,27} The iterative extended Hückel theory (IEHT) method was used to test both oxidized and reduced states of several conformers of $\text{Fe}(\text{SH})_4$. For each conformer of the oxidized model the energies of several different d^5 configurations were calculated.

In extended Hückel theory, there are no two-electron integrals and hence, states of the same occupation but different overall spin are energetically indistinguishable. Thus sextet, quartet, and doublet states with the same d^5 configuration are equal in energy. This is, of course, an extremely serious limitation for studies of Rd models which Loew and co-workers attempt to remove by ad hoc means. Namely, after calculating the orbitals, they add to the extended Hückel energy a correction term of the same form as the exchange part of the two-electron energy. This will decrease the energy of high-spin states with respect to low-spin states and hence modify the energies in the direction of the ab initio results. In the Rd models, the various d^5 (or d^6) configurations are no longer equivalent (as for the atom), and consequently extended Hückel theory will generally favor occupations with doubly occupied orbitals. (In ab initio calculations these states are many electron volts above the ground state.) Unfortunately, even using exchange integrals corresponding to an orbital ten times as tight as an Fe 3d orbital does not correct the IEHT sufficiently to provide correct atomic splittings. In addition, since the experimental sextet to quartet splitting in Rd is not known, Loew and co-workers could not determine the magnitude of the necessary exchange correction for their models. Instead they adjusted the integrals to obtain degeneracy of the sextet and lowest quartet states, and then in their spin-orbit and spin-spin properties the sextet-quartet separation was treated as an adjustable parameter of the order of 0.1 eV. Our ab initio calculations show the lowest quartet state to be 0.98 eV above the sextet ground state (10 times the assumed separation in the IEHT studies). Therefore the good agreement with experiment of the spin-spin and spin-orbit properties of the IEHT calculations is irrelevant.

C. Redox Potential. Since Rd is an electron transfer enzyme, its redox potential is the salient electronic property. There are several difficulties and little experience in abstracting such quantities from electronic wave function calculations but we have proceeded as follows.

The redox potential is just the ionization potential (IP) of the reduced state referenced with respect to the standard hydrogen electrode, so we must first consider the IP of our complex. Considering just the bare $\text{Fe}(\text{SH})_4$ model the calculated IP for reduced to oxidized, i.e.,



is -1.67 eV; however, this number does not pertain directly to either Rd or its models. The problem is that in both the protein and in solution the FeS_4 moiety is surrounded by a dielectric medium that is polarized by the charged FeS_4 unit,

Table IV. The Redox Potential^a for the Rd Model

| radius of charged complex, Å ^b | | dielectric constant ε | correction for infinite potential, eV | | redox potential, eV ^c |
|---|---------|--------------------------|---------------------------------------|---------|----------------------------------|
| oxidized | reduced | | oxidized | reduced | |
| 3.497 | 3.586 | 10 | -1.85 | -7.23 | -0.79 |
| 3.597 | 3.686 | 10 | -1.80 | -7.03 | -0.94 |
| 3.697 | 3.786 | 10 | -1.75 | -6.85 | -1.07 |
| 3.497 | 3.586 | 37 | -2.00 | -7.81 | -0.36 |
| 3.597 | 3.686 | 37 | -1.95 | -7.60 | -0.52 |
| 3.697 | 3.786 | 37 | -1.89 | -7.40 | -0.66 |
| 3.497 | 3.586 | 80 | -2.03 | -7.93 | -0.27 |
| 3.597 | 3.686 | 80 | -1.98 | -7.72 | -0.43 |
| 3.697 | 3.786 | 80 | -1.92 | -7.51 | -0.58 |

^a CI calculations give an IP of -1.67 eV for the reduced model. ^b Reduced size = oxidized size + 0.089 Å (the difference in Fe-S distance in the Holm models, ref 4). ^c Relative to Pt/H₂ electrode (this corresponds to an IP of ~4.5 eV).

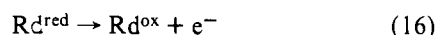
with the polarization energy changing markedly upon ionization. To estimate this effect we proceeded as follows.

Consider that the Fe(SH)₄²⁻ or Fe(SH)₄⁻ unit is immersed in an appropriate dielectric medium representing the protein or solvent. We can estimate the additional effect of polarization of the rest of the protein or solvent by considering the polarization of the dielectric medium due to a point charge at the center of a hollow sphere having the radius of our complex.

$$U = -\frac{1}{2} \left(\frac{\epsilon - 1}{\epsilon} \right) \frac{e^2}{r_0} \quad (15)$$

where U is the induced potential, ϵ is the dielectric constant of the solvent, e is the charge, and r_0 is the size of the sphere. Using $r_0 = 3.686$ Å for the reduced model and 3.597 Å for the oxidized model (the Fe-S distance plus the S-H distance), and $\epsilon = 37$ to represent the solvent²⁸ DMF, the corrections are -1.95 eV for the oxidized state and -7.60 eV for the reduced state. Thus the calculated IP of -1.67 eV is corrected to a value of +3.98 eV for the Fe(SH)₄ unit in an infinite medium.

Now we must convert our calculated IP into the standard scale for redox potentials. Lohmann²⁹ has estimated that the conversion of the redox potential (relative to the standard hydrogen electrode) to an absolute IP scale involves an additive constant of -4.5 eV. Thus the calculated IP of our complex (3.98 eV) leads to a redox potential of -0.52 eV for



This compares with -0.057 eV for Rd³⁰ and -0.8 ± 0.3 eV estimated for the Holm compound.³¹ The values obtained with other choices of ϵ and the hole radius r_0 are tabulated in Table IV.

VI. Summary

In what we believe is the most extensive ab initio theoretical study of the electronic structure of a transition metal complex, we have found the following.

(1) Reduced Rd model: (a) The ground state is high spin (quintet), with a d⁶ configuration (d_{z²} doubly occupied). (b) The lowest triplet d⁶ excited state is at 2.79 eV while the lowest singlet excited state is at 4.03 eV. (c) The orientation of the S-H groups splits the usual tetrahedral levels ⁵E and ⁵T₂ (with ⁵E lower) into ⁵E components at 0 and 0.17 eV and ⁵T₂ levels at 0.32, 0.61, and 0.62 eV. (d) Averaging these levels leads to a tetrahedral ligand field splitting of $\Delta = 10Dq = 0.43$ eV = 3500 cm⁻¹, which is about 80% of the value for aquo-oxygen ligands. (e) The d-d spin-forbidden transitions lie at 2.6-3.0 eV (observed ϵ 390 M⁻¹ cm⁻¹).

2. Oxidized Rd model: (a) The ground state is high spin (sextet) with the lowest quartet state at 0.98 eV and the lowest doublet state at 2.76 eV. (b) The ground state is a mixture of two sextet states, (i) Fe^{III}L₄⁴⁻ where the ligands are as in re-

Table V. Comparison of SCF and CI Results for Quintet States of the Reduced Model

| state | d configuration | | | | | Fe(SH) ₄ ²⁻ geometry C ^a | |
|-------|-----------------|----------------|----|----|----|---|---------------------|
| | z ² | y ² | xy | yz | xz | SCF, ^b eV | CI, ^c eV |
| I | 2 | 1 | 1 | 1 | 1 | 0 | -0.01 |
| II | 1 | 2 | 1 | 1 | 1 | 0.37 | 0.36 |
| III | 1 | 1 | 2 | 1 | 1 | 0.52 | 0.53 |
| IV | 1 | 1 | 1 | 2 | 1 | 0.72 | 0.72 |
| V | 1 | 1 | 1 | 1 | 2 | 0.80 | 0.80 |

^a This geometry differs from the reduced model described in this work; see ref 17. ^b Total energies SCF = -65.2554 hartrees; CI = -65.2559 hartrees. ^c CI calculation included all single excitations from the five d configurations above, excluding those from ligand orbitals to d virtual orbitals. The CI basis is analogous to that described in the Appendix.

duced Rd and the d configuration is high spin d⁵ and (ii) Fe^{II}L₄³⁻ where a delocalized ligand orbital has been oxidized. This state is a mixture of several configurations so as to lead to a nearly spherical charge distribution. (c) The transition observed at 1.66 eV (ϵ 360 M⁻¹ cm⁻¹) is d-d spin forbidden. (d) Ligand to metal charge transfer (LMCT) occurs at 2 and 2.5 eV where the lower band includes transitions into e-like orbitals while the higher band includes transitions into t₂-like orbitals.

Appendix. Details of the CI Calculations

A. The CI Basis. In these calculations the CI basis consisted of 26 functions. Since the Ar core of Fe and the Ne core of S were replaced by effective potentials, there were 21 occupied valence orbitals in both the oxidized and reduced SCF (done at the HF level). For the reduced CI basis, the valence orbitals were obtained from a high-spin quintet calculation where the d orbitals were spherically averaged (each of the five d orbitals had 1.2 electrons). This approach was tested and found to produce a basis well suited for all five quintet states (see Table V). The oxidized CI basis came from the high-spin sextet SCF calculation. The four S(3s) orbitals were not always included in the CI basis, since our past experience has shown that excitations from these orbitals are of little importance in the relative energies of the kind of states we examined here. To the 21 valence orbitals a set of five diffuse d orbitals was added to allow important size readjustments in the d orbitals as the orbital occupation changes from state to state. Thus the final CI basis consisted of 26 orbitals, 16 valence ligand orbitals, 5 valence d orbitals, and 5 virtual d orbitals. The following sections describe in detail the configurations used in each of the six CIs. This approach was developed after numerous tests of

the effects of various restrictions in the CI wave function. No symmetry restrictions were used.

B. The CI Calculations for Reduced States. 1. Quintet States. The basic configuration list for the quintet reduced states starts with all configurations having 42 ligand electrons [four (SH)⁻] and 6 d electrons in the Fe valence d orbitals, and all those with 41 ligand electrons and 7 d electrons (allowing single excitations from ligand to metal). Using this configuration list, single excitations from each of the five d orbitals into the corresponding d virtual orbital were allowed. To the above list, all configurations involving the excitation of two electrons from the ligands [excluding S(3s)] to the d orbitals were added. Overall, we have allowed all single excitations in the valence space, along with single excitations from the d orbitals into virtuals and finally some ligand to metal double excitations. The final list included 1450 spatial configurations or 2430 spin eigenfunctions (2675 determinants).

2. Triplet States. For the triplet states, we started with all configurations having a filled ligand space (42 electrons) and six valence d electrons. This represents a full CI over the five valence d orbitals. To this list all excitations from each of the five d orbitals into the corresponding d virtual orbital were allowed. Finally, all single excitations from the ligand orbitals [excluding the S(3s)] into the valence d orbitals were added. So again we have allowed all single excitations among the valence orbitals from all of the 35 possible d⁶ triplet configurations. In addition, the d orbitals can readjust their shape through excitations involving the d virtuals. This CI calculation is not quite as extensive as the one for quintet states, but it does adequately describe the important CI effects. Results for this CI were in good agreement with triplet SCF calculations done on another geometry, supporting the use of the basis set from a quintet HF calculation to solve for triplet CI wave functions. The final configuration list contained 540 spatial configurations or 990 spin eigenfunctions (1225 determinants).

3. Singlet States. The singlet configurations were generated in exactly the same way as the triplet configurations. The final list had 580 spatial configurations or 805 spin eigenfunctions (2060 determinants).

C. The CI Calculations for Oxidized States. 1. Sextet States (Including LMCT). In the reduced wave functions only five occupied orbitals were predominantly of Fe d character. However, in the sextet oxidized SCF calculation, one of the ligand orbitals (σ to the Fe) mixed in a significant portion of d character. Likewise, one of the singly occupied Fe d orbitals contained a significant amount of ligand character. Since six occupied orbitals have extensive d character, we must be very careful in the CI to allow the electrons in all six orbitals to readjust in mutual response to various CI excitations. Consequently we started with the set of all single and double excitations from the ligand orbitals [S(3s) excluded] into the six d-like orbitals. As in the other CIs, single excitations were allowed from occupied d orbitals to virtual d orbitals using each of the above configurations. Thus the final list of 1741 spatial configurations contained d⁵, d⁶, and d⁷ configurations. This configuration list proved entirely adequate for describing both the ground state and LMCT transitions.

2. Quartet States. We decided to solve only for the lowest seven quartet states. We started with a full CI over the six orbital valence d space, then added all single excitations from the ten most important d configurations (now considering all 21 valence orbitals). Then excitations from the d orbitals into the corresponding d virtuals were added. This produced the 571 configurations necessary to describe the seven lowest quartet states (1510 spin eigenfunctions or 1823 determinants).

3. Doublet States. The doublet states were done in exactly the same manner as the quartets, this time using the six most important configurations as the starting point for single excitations among the valence orbitals. Since only the lowest root was desired, the final list of 869 configurations proved adequate (2466 spin eigenfunctions or 4349 determinants).

References and Notes

- (1) Computing assistance was obtained from the Health Sciences Computing Facility of the University of California, Los Angeles, supported by the National Institutes of Health, Research Resources Grant RR-3. This work was partially supported by NIH Research Grant GM-23971 from the National Institute of General Medical Sciences.
- (2) National Institutes of Health Trainee, 1977-1978.
- (3) See, for example, the following reviews: W. Lovenberg, Ed., "Iron-Sulfur Proteins", Vol. 1-3, Academic Press, New York, N.Y., 1973, 1973, and 1977; G. Palmer, "The Enzymes", Vol. 12, 3rd ed, P. D. Boyer, Ed., Academic Press, New York, N.Y., 1975, p 1; W. H. Orme-Johnson, *Annu. Rev. Biochem.*, **42**, 159 (1973); M. Llinas, *Struct. Bonding (Berlin)*, **17**, 176 (1973).
- (4) R. W. Lane, J. A. Ibers, R. B. Frankel, G. C. Papaefthymiou, and R. H. Holm, *J. Am. Chem. Soc.*, **99**, 84 (1977).
- (5) D. Coucouvanis, D. Swenson, N. C. Baenziger, D. G. Holah, A. Kostikas, A. Simopoulos, and V. Petrouleas, *J. Am. Chem. Soc.*, **98**, 5721 (1976); D. Coucouvanis, D. G. Holah, and F. J. Hollander, *Inorg. Chem.*, **14**, 2657 (1975).
- (6) J. R. Anglin and A. Davison, *Inorg. Chem.*, **14**, 234 (1975).
- (7) (a) K. D. Watenpaugh, L. C. Sieker, J. R. Herriott, and L. H. Jensen, *Acta Crystallogr., Sect. B*, **29**, 943 (1973); (b) L. H. Jensen, private communication; see ref 7d; (c) D. E. Sayers, E. A. Stern, and J. R. Herriott, *J. Chem. Phys.*, **64**, 427 (1976); R. G. Shulman, P. Eisenberger, W. E. Blumberg, and N. A. Stombaugh, *Proc. Natl. Acad. Sci. U.S.A.*, **72**, 4003 (1975); (d) B. Bunker and E. A. Stern, *Biophys. J.*, **19**, 253 (1977).
- (8) Open-shell HF calculations used the method of W. J. Hunt, W. A. Goddard III, and T. H. Dunning, Jr., *Chem. Phys. Lett.*, **6**, 147 (1970).
- (9) A. J. Wachtors, *J. Chem. Phys.*, **52**, 1033 (1970).
- (10) C. F. Melius, B. D. Olafson, and W. A. Goddard III, *Chem. Phys. Lett.*, **28**, 457 (1974); M. J. Sollenberger, M.S. Thesis, California Institute of Technology, 1975.
- (11) R. A. Bair and W. A. Goddard III, unpublished results.
- (12) S. Huzinaga, *J. Chem. Phys.*, **42**, 1293 (1965).
- (13) POLYATOM is Quantum Chemistry Program Exchange No. 189.
- (14) The GVB method is described in W. A. Goddard III, T. H. Dunning, Jr., W. J. Hunt, and P. J. Hay, *Acc. Chem. Res.*, **6**, 368 (1973), and references cited therein; see F. W. Bobrowicz and W. A. Goddard III, "Modern Theoretical Chemistry: Methods of Electronic Structure Theory", Vol. 3, H. F. Schaefer III, Ed., Plenum Press, New York, N.Y., 1977, pp 79-127, for a detailed discussion.
- (15) W. D. Phillips, M. Poe, J. F. Weiher, C. C. McDonald, and W. Lovenberg, *Nature (London)*, **227**, 574 (1970).
- (16) K. K. Rao, M. C. W. Evans, R. Cammack, D. O. Hall, C. L. Thompson, P. J. Jackson, and C. E. Johnson, *Biochem. J.*, **129**, 1063 (1972).
- (17) R. A. Bair and W. A. Goddard III, *J. Am. Chem. Soc.*, **99**, 3505 (1977).
- (18) W. A. Eaton and W. Lovenberg in "Iron Sulfur Proteins", Vol. 2, W. Lovenberg, Ed., Academic Press, New York, N.Y., 1973, Chapter 3.
- (19) W. A. Eaton, G. Palmer, J. A. Fee, T. Kimura, and W. Lovenberg, *Proc. Natl. Acad. Sci. U.S.A.*, **68**, 3015 (1971).
- (20) A. Davison and E. S. Switkes, *Inorg. Chem.*, **4**, 837 (1971).
- (21) J. Peisach, W. E. Blumberg, E. T. Lode, and M. J. Coon, *J. Biol. Chem.*, **246**, 5877 (1971).
- (22) J. Rawlings, O. Silman, and H. B. Gray, *Proc. Natl. Acad. Sci. U.S.A.*, **71**, 125 (1974).
- (23) The experimental estimates of intensity have some uncertainty in subtracting background and in line shape idealizations. Theoretical values within a factor of 2 would be considered good agreement for this level of calculation.
- (24) J. G. Stevens and B. D. Dunlap, *J. Phys. Chem. Ref. Data*, **5**, 1093 (1976).
- (25) J. G. Norman, Jr., and S. C. Jackels, *J. Am. Chem. Soc.*, **97**, 3833 (1975).
- (26) G. H. Loew and D. Y. Lo, *Theor. Chim. Acta*, **32**, 217 (1974); G. H. Loew, M. Chadwick, and D. A. Steinberg, *ibid.*, **33**, 125 (1974).
- (27) G. H. Loew and D. Lo, *Theor. Chim. Acta*, **33**, 137 (1974); G. H. Loew, M. Chadwick, and D. Lo, *ibid.*, **33**, 147 (1974).
- (28) G. H. Brown and R. Al-Urfali, *J. Am. Chem. Soc.*, **80**, 2113 (1958).
- (29) F. Lohmann, *Z. Naturforsch. A.*, **22**, 843 (1967).
- (30) W. Lovenberg and B. E. Sobel, *Proc. Natl. Acad. Sci. U.S.A.*, **54**, 193 (1965).
- (31) The value of -0.8 ± 0.3 eV was obtained by taking Holm's measured value of -1.03 eV relative to a standard calomel electrode (SCE) in DMF (ref 4) and adjusting it by 0.25 eV for the difference in the SCE in aqueous solution relative to the standard hydrogen electrode. This correction is considered approximate since the properties of the SCE differ in aqueous vs. non-aqueous (DMF) solvents.